



OPEN

Pollution indices of brackish water and sediments of major mangrove sites along Arabian Sea coast of Pakistan

Malik Wajid Hussain Chan¹, Muhammad Ibrahim², Muhammad Qasim³, Manzer. H. Siddiqui⁴, Saud Alamri⁴, Pirzada Jamal Ahmed Siddiqui¹, Salman Gulzar³, Muhammad Azeem⁵, Troy T. Handlovic⁶, M. Farooq Wahab⁶, Alanoud T. Alfangham⁴ & Munawwer Rasheed^{1,7}✉

Heavy metal (HM) contamination poses a significant environmental threat to Mangrove ecosystems, particularly in industrial and urban-influenced regions. This study has investigated the spatial and seasonal distribution of HM in water and sediment samples from three major mangrove sites along the Arabian Sea coast of Pakistan, Indus Delta, Sandspit and Miani Hor. Ten heavy metals (HM)- aluminum (Al), arsenic (Ar), cadmium (Cd), chromium (Cr), copper (Cu), iron (Fe), lead (Pb), mercury (Hg), selenium (Se), and zinc (Zn) were assessed using multiple pollution indices to evaluate the contamination levels and ecological risks. Multivariate analysis (MANOVA) and principal component analysis (PCA) revealed significant effects of sample types (water and sediments), sites, and seasons on HM concentrations. Sandspit exhibited the highest pollution level primarily due to industrial discharge and wastewater influx. Pollution indices identified Sandspit as the most contaminated mangrove stand. In seawater, HM Contamination factor (C_f) followed the order: Hg > Cr > Al > Pb > As > Cd > Fe > Cu > Zn > Se, whereas individual Heavy Metal Pollution Index (HPI) sequence was Hg > Cd > Al > Pb > Cr > As > Cu > Fe > Se > Zn. Seasonal variations, especially during the monsoon, intensified HM mobilization, further deteriorating water quality. The excessive Hg levels surpass national and international safety limits, posing ecological and public health risks. The prolonged retention of Cd, Cu, and Al in sediments indicates persistent contamination affecting mangrove vegetation and associated marine biodiversity. Urgent intervention is required to regulate industrial waste, improve pollution control, and implement sustainable remediation strategies to protect coastal ecosystems.

Keywords Heavy metals pollution indices, Indus delta, Mangrove ecosystem, Miani Hor, Monsoon, Sandspit, Seasonal variations

Mangrove stands are crucial for sustaining biodiversity, providing habitats for various species, including fish, birds, and endangered marine mammals. Mangrove ecosystems act as natural barriers against coastal erosion and help mitigate climate change by sequestering carbon. They support local economies through eco-tourism and serve as nursery grounds for commercially valuable fish species. Mangroves are also a source of products that support the local economy, such as black tea, mosquitocides, gallotannins, microbial fertilizers, antiviral drugs, and UV-blocking compounds. Additionally, mangroves enhance water quality by filtering pollutants and trapping sediments, thereby protecting more sensitive marine habitats downstream¹. Mangrove soils and sediments trap heavy metals (HM) through organic ligation, protecting coastal marine environments from pollution². Therefore, the water and sediment surrounding mangroves are an excellent location to study environmental pollutants when evaluating the fate and risk that these pollutants pose to the surrounding ecosystems and biota.

¹Centre of Excellence in Marine Biology, University of Karachi, Karachi 75270, Pakistan. ²Pakistan Standards and Quality Control Authority, Block-77, Pakistan Secretariat, Karachi 74400, Pakistan. ³Dr. Muhammad Ajmal Khan Institute of Sustainable Halophyte Utilization, University of Karachi, Karachi 75270, Pakistan. ⁴Department of Botany and Microbiology, College of Science, King Saud University, P.O. Box 2455, Riyadh 11451, Saudi Arabia. ⁵Department of Botany, University of Karachi, Karachi 75270, Pakistan. ⁶Department of Chemistry and Biochemistry, University of Texas at Arlington, Arlington, TX 76019, USA. ⁷Department of Chemistry, University of Karachi, Karachi 75270, Pakistan. ✉email: rasheed.munawwer@uok.edu.pk

Pakistan has an estimated 240,000 sq. km. of marine area with a coastline of about 1,050 km along the Northern Arabian Sea. At one time, Pakistan had eight mangrove species: *Bruguiera conjugata*, *Ceriops roxburghiana*, *C. tagal*, *Rhizophora apiculata*, *R. mucronata*, *Aegiceras corniculata*, *Avicennia marina*, and *Sommeratia caseolaris* with *A. marina* being the most abundant species³. However, over-exploitation, pollution, decline in fluvial discharge into the Indus Delta, and changes in the environmental conditions have made four of these extinct from Pakistani coast⁴. Over 269 million gallons per day of industrial waste and sewage from Karachi are discharged, primarily entering the Arabian Sea through Lyari and Malir Rivers. These rivers also receive terrestrial runoff during the rainy monsoon season⁵. To evaluate the levels of HM in the brackish water and sediments in mangrove stands, three geographically diverse locations in Pakistan near the Arabian Sea were sampled: (i) Sandspit, (ii) Miani Hor, and (iii) Indus Delta (Fig. 1). Sandspit backwaters are situated at the mouth of Karachi and comprise a monospecific mangrove stand of *A. marina*⁶. Sandspit is flooded periodically with ~ 3.4 million m³ of seawater from the Arabian Sea through the Manora channel⁷. Reported data suggest that 92% of urban wastewater and 99% of industrial effluents are discharged untreated, causing environmental stress in urban areas of Pakistan⁸. Miani Hor, along the Balochistan coast, is a protected lagoon with a mangrove cover of 31 km² and contains about 2% of the total mangrove population in Pakistan⁴. Here, *A. marina*, *C. tagal*, and *R. mucronata* co-exist⁹. Miani Hor receives run-off discharge during monsoon from two ephemeral rivers, the Porali and Winder. The Indus River delta extends eastward to the Indian border and is ranked the world's fifth largest mangrove forest (0.26 million hectares). These dense mangrove forests are dominated by *A. marina* (98%) with small populations of *R. mucronata*, *C. tagal*, and *A. corniculatum*¹⁰. Indus Delta and Miani Hor are declared as Ramsar sites⁴.

HM impart adverse effects on the water quality, benthic biota, and other organisms. HM are persistent pollutants since these can penetrate the sediments and resist decomposition in natural conditions¹¹. Thus, sediments are a potential source for the HM that accumulate in the tissues of marine biota and ultimately enter the food chain. An extended stay of HM in water columns also develops severe environmental risks^{12,13}. Water bodies act as a “mobile phase” for the dissolved HM to move within these columns. In the mangrove ecosystem, HM ions form soluble complexes with organic and inorganic ligands before being absorbed and accumulated in mangrove tissues, causing long-term damage¹⁴. *A. marina* exhibit higher HM tolerance than the other species and thus are most abundant¹⁵. In the current study, the distribution of ten HM namely aluminum (Al), arsenic (Ar), cadmium (Cd), chromium (Cr), copper (Cu), iron (Fe), lead (Pb), mercury (Hg), selenium (Se), and zinc (Zn) present in water and sediment of three well-separated mangrove sites along the Arabian Sea coast were assessed during three different seasons (pre-monsoon, monsoon and post-monsoon). The HM Pollution Indices (HPI), Contamination Degrees (C_d), Modified Contamination Degrees (mC_d), Enrichment Factors (EF), Geo-accumulation Indices (I_{geo}), Pollution Load Indices (PLI), Contamination Factors (C_f), and Potential

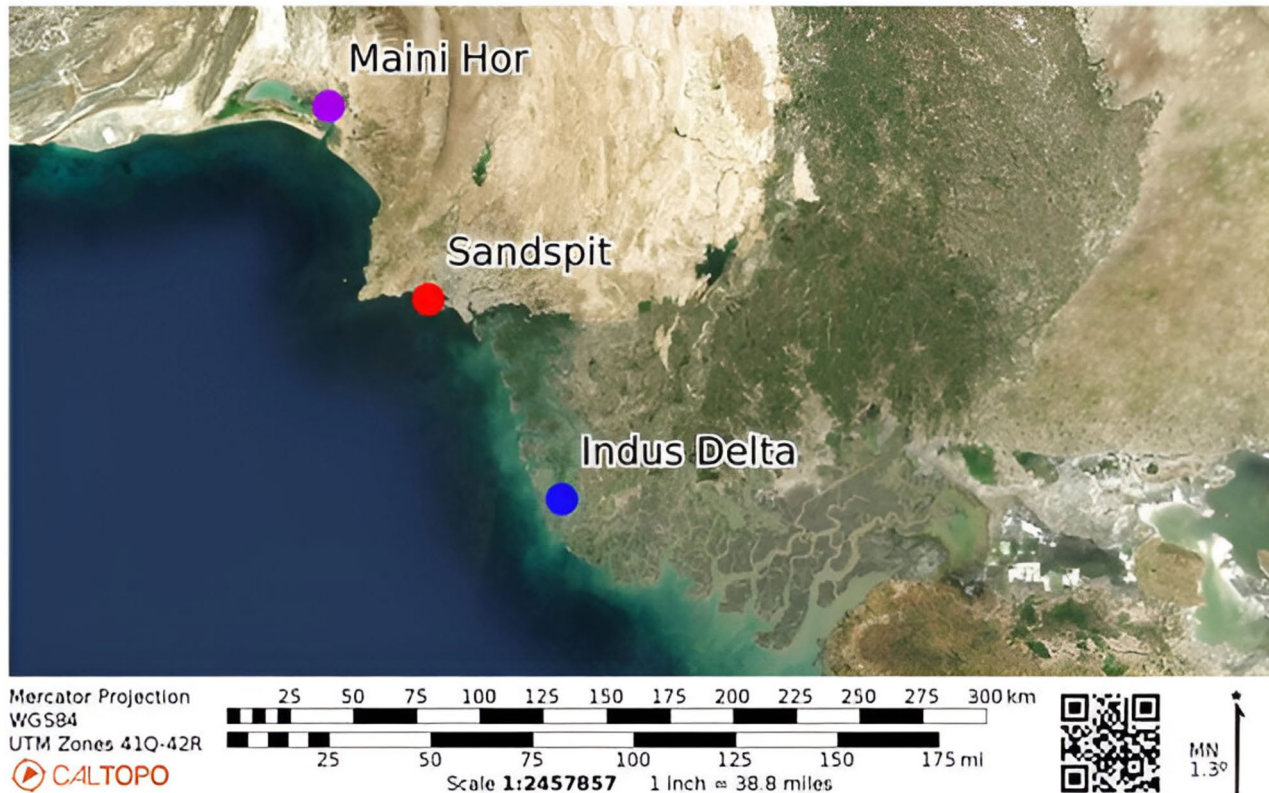


Fig. 1. Colored circles indicate the sampling sites along the North Arabian Sea coast of Pakistan. The image is sourced from the <https://caltopo.com/map.html>.

Ecological Risk Indices (Eri^i) were evaluated to support the experimental data. Multivariate Analyses of Variance (MANOVA) was conducted to find out the significant differences. Principal component analysis (PCA) was conducted to see if grouping appears in site locations, seasons, and water or sediments. It was hypothesized that the pollution levels would be higher (1) during pre-monsoon and (2) at Sandspit.

Materials and methods

Study sites

Three different mangrove sites (Fig. 1) were selected for pollution assessment. These included Indus delta ($24^{\circ} 93' 33''$ N, $67^{\circ} 27' 43.54''$ E), Sandspit backwater ($24^{\circ} 49' 49''$ N, $66^{\circ} 55' 41''$ E), and Miani Hor Bay ($25^{\circ} 30' 55.76''$ N, $66^{\circ} 32' 29.41''$ E). A hand-held global positioning system (GPS) tracked the locations.

Sample collection and preparation

Replicates (3–5) of water and sediment were sampled from a depth of 5 to 7 cm around the pneumatophores/roots of mangroves during the monsoon (Jun to Sep 2017), post-monsoon (Oct to Nov 2017) and pre-monsoon (Mar to May 2018) seasons at the start of ebbing during a single low tide. The water samples were collected in 1 L acid-washed clean plastic bottles while the sediments were stored in clean polyethylene zip-locked bags. During traveling, samples were stored in an ice box and processed immediately for analysis. Known volumes of water samples were kept in a water bath at 30 to 40 °C for evaporation until the salt was obtained, replicating the salt pan process¹⁶. The air-dried samples of salts and sediments were ground to powder using mortar and pestle. Weighed amounts of each sample of powdered salt (± 0.5 g) and sediments (± 2.0 g) was digested using fuming nitric acid in acid-resistant vessels. The volumes of digested samples, primarily made up to 50 mL in deionized water, were filtered through Whatman filter paper no. 42, and analysed. If not found within the calibration range, secondary dilutions were prepared accordingly¹⁷. The range of calibration curves used for analysing Cd, Cu, Se, and Zn were from 0 to 10 mg·L⁻¹, while for other HM it was from 0 to 100 mg·L⁻¹.

Heavy metal analyses using atomic absorption spectrophotometry

Metal concentrations were determined using an atomic absorption spectrophotometer (Agilent series 200). To detect each HM, a single beam hollow cathode lamp of Hg, Cd, As, Pb, Cu, Cr, Zn, Fe, Al, and Se were used at specific wavelengths. Flame atomization (240 FS AA) was used for the detection of Cu, Fe, and Zn; graphite tube atomization (240Z AA) for the analysis of Al, As, Cd, Cr, Pb, and Se; and vapor generation accessory (77A) for the analysis of Hg. Standard solutions obtained from Sigma Aldrich including Hg (cat. no. 16482), Cd (cat. no. 51994), As (cat. no. 39436), Pb (cat. no. 16595), Cu (cat. no. 38996), Cr (cat. no. 02733), Zn (cat. no. 18827), Fe (cat. no. 16596), Al (cat. no. 39435), Se (cat. no. 89498), were used to prepare calibration curves.

Ecological and environmental indices and factors

The calculations and equations of all the indices and factors used in this study is available in supplementary data file.

Statistical analysis

Data obtained from the analysis were expressed as mean \pm standard deviation (SD). Samples analyzed had a Relative Standard Deviation (RSD) of 1–5%. Data have been tested for homogeneity in variation before being analyzed for multivariate analysis (MANOVA). Principal Component Analysis (PCA) was carried out using MATLAB (The MathWorks Inc., MA, USA) version R2023a. The results were analyzed using Microsoft Excel (ver. 10). All statistical calculations were performed using SPSS® ver. 23.0 (Chicago, IL, USA). Paleontological statistics (PAST®, Version 3.21) was used to analyze similarity index and cluster analysis.

Results and discussion

Environmental considerations for site selection

Three sites (Fig. 1) were selected due to their geospatial characteristics. Sandspit is a sandy beach, but its backwaters are exposed to domestic waste and industrial discharge from the Lyari River. The area is a complex of coastal wetlands and contains shallow tidal lagoons, intertidal mudflats, saltfans, estuaries, saline ponds, mangrove swamps, clay, and some sandy patches. Miani Hor is a swampy lagoon. The sediment is alluvial, composed of light, loose clay mixed with fine sand and saline ingredients. The main minerals are shale, marble, limestone, barite, and serpentine¹⁸. Alluvium is typically made up of various materials, from fine particles of silt and clay to larger particles of sand and gravel and often contains a good deal of organic matter. High alluvial deposits were observed in these sediments¹⁹. Indus River brings the silt to the delta. Indus Delta sediment is entirely alluvial, with fine silt, clay, and lesser shale material. Further westward of the delta, the shelf sediments change from silt to fine sand²⁰.

Furthermore, these sites are affected by meteorological conditions, as tidal directions change frequently during the monsoon season and become aggressive. Higher water and fuel consumption during the summer increases pollutant discharge into seawater, leading to higher chemisorbed HM sediment levels. Drilling mud from local mining further contributes to HM accumulation²¹. In Balochistan, drilling for mining causes HM pollution in seawater and sediments. Drilling mud is usually a powder of heavy minerals, e.g., ilmenite, haematite, galena, and barite²². A natural monospecific *A. marina* stand in the Sandspit backwaters can thrive with untreated wastewater frequently inundated with seawater. The decline in mangrove species diversity indicated that the area is under severe pollution stress and only *A. marina* is surviving. It was also observed during field visits that pollution levels is affecting the mangroves environment, resulting in stunted growth. Besides HM stress, other factors, e.g., low freshwater intake and high salinity, also influence their development.

Increasing water pollution has also burdened the Indus Delta. Natural processes such as erosion and human activities, such as agriculture, industrial effluents, mining, etc., introduce synthetic chemicals, fertilizers, pesticides, and toxic metals into surface and groundwater resources. These are possibly the leading cause of HM pollution in the Indus River, which finally runs into the Arabian Sea²³. Freshwater from the Indus River dilutes but pollutes the delta. Stunted growth of mangroves was also observed²⁴.

Multivariate analysis of variance (MANOVA)

The MANOVA results indicate that sample types, sites, and seasons significantly influence HM concentrations, as strong interactive effects have been reflected among these factors (Supplementary File, Table S1). Sample types (water and sediment) shows a highly significant impact on most HMs, indicating distinct physicochemical processes governing metal retention and mobility. Significant site-specific differences demonstrate that pollution levels are not uniform across Indus Delta, Sandspit, and Miani Hor, likely due to differences in natural geochemical characteristics, hydrodynamic conditions, and anthropogenic activities. Seasonal variations significantly affect multiple HM, likely due to the dynamic nature of metal distribution, which could be attributed to variations in monsoonal rainfall, tidal influences, sediment transportation and climatic conditions. The interactions between sample types, sites, and seasons are highly significant, emphasizing that metal distribution is not uniform but rather influenced by a combination of environmental and geographical factors. The results highlight the complex nature of HM contamination and underscore the need for site- and season-specific approach in monitoring and managing HM pollution in mangroves ecosystems.

Principal component analysis

PCA provides a means of dimensionality reduction and visualization of elemental composition rather than a direct significance test. PCA was performed to investigate the elemental composition and grouping of water samples from the three areas shown in Fig. 1 across different seasons (pre-monsoon, monsoon, and post-monsoon). PCA was performed on z-scores of the data in Table 1 to address the varying range and distribution of HM concentrations. We focus on the first two principal components (PC1 and PC2), which explain $78.9 + 14.0 = 92.9\%$ of the variance in water (Fig. 2A,B) and $65.5 + 19.8 = 85.3\%$ in sediment (Fig. 2C,D). Sandspit (Fig. 2A, red) is distinctly separated along PC1, indicating a unique HM profile compared to Miani Hor and Indus Delta. This separation is primarily influenced by strong positive loadings on PC1 of tested HM except Hg and Se (Fig. 2B). Indus Delta (blue dots) and Miani Hor (green dots) cluster more closely together, indicating similar elemental compositions (Fig. 2B). These locations show variations primarily along PC2 (Fig. 2A). The PC2 loadings indicate heavy influence due to Hg, As, and Se. PC1 captures high variance and highlights the dominance of elements like Pb in distinguishing water quality at Sandspit, while PC2 differentiates Indus Delta and Miani Hor based on secondary HM variations. Overall, the PCA results visualize spatial differences in water quality, driven by varying concentrations of critical HM across not only locations but also seasons.

It was further desired to see the grouping of sampling sites on the sediments at the three designated locations since they may serve as adsorption sites for the various HM species. As seen in Fig. 2C, the sediments show notable grouping on PC1 and PC2. PC1 captures 65.5% of the variance with positive loadings for all elements except Hg, Cd, As, Cu, Cr, Zn, and Fe contribute almost the same to the linear combination of PC1. The second PC axis captured 19.8% variance with Hg, Al, and Se having large positive loadings and an almost equal negative loading from Cd and Fe (Fig. 2D). It appears that seasons had relatively less influence on the sediments' HM composition than site, implying that they stick to the solids in the mangroves, as observed in Malaysian mangroves²⁵.

This analysis highlights the importance of seasonal monitoring and the need for targeted remediation strategies tailored to the specific HM profiles of each location, as shown in Table 1. The cluster analysis of sediment samples made a cluster between Miani Hor and Indus Delta, showing similarity (0.89). Sandspit shows a value of 0.76 and 0.68 with Miani Hor and Indus Delta, respectively. The same observation is true with water analysis shown in the dendrogram (Supplementary File, Fig. S1). Study sites fall into two clusters: one consisting of Miani Hor and Indus Delta, and the second being Sandspit (Fig. 2B). These dendrogram results also support the MANOVA findings (Supplementary File, Table S1) that location plays a significant role in HM accumulation profiles, whereas PCA simply provides a graphical representation of those variations.

Hg analysis

Hg is a highly toxic metal, causing neurological, cardiovascular collapse, renal failure, and gastrointestinal damage. Mercury vapors are easily transported into the atmosphere and ultimately fall into the aquatic environment, entering the human food chain²⁶. In this study, MANOVA revealed significant effects of sample types, sites, seasons and their interactions on Hg accumulation (Supplementary File, Table S1). In the current work, water samples contained significantly higher levels of Hg (Table 1) than sediment samples (Table 2). Both water and sediment samples exhibited a similar trend in all studied sites, with the highest Hg concentration observed during the monsoon and the lowest during the pre-monsoon. The average Hg content in these sites was comparable but exceeded the standard limits. The percentage difference ($\% \Delta$) from the National Environmental Quality Standards (NEQS)²⁷ was notably high in water, i.e., 142,100, 143,200, and 116,800, and in sediment, i.e., 2710, 2850, and 2425 at Sandspit, Indus Delta and Miani Hor, respectively (Tables 1, 2). Estuaries and coastal regions are particularly susceptible to anthropogenic Hg contamination, which can enter the marine environment through atmosphere or discharge directly from water bodies²⁸. The effects of tides could explain this relatively even distribution. Similar observations have also been reported by Byrd²⁹. In this study, solid–liquid distribution coefficients (K_d), ranged from 0.73 to 0.90, indicating higher retention of Hg in water compared to sediment³⁰.

The high Hg content is alarming and has been documented by various research groups^{22,31}. Extensive data on the Hg assessment in seawater is available, reaching levels as high as 3 ppm^{32–34}. On a global scale, assessment of

HM	NEQS, 1997	Sandpit			Miani Hor			Indus Delta								
		Monsoon	Post-monsoon	Pre-monsoon	Average	% Δ^*	Monsoon	Post-monsoon	Pre-monsoon	Average	% Δ^*	Monsoon	Post-monsoon	Pre-monsoon	Average	% Δ^*
Hg	<0.01	16.5 \pm 0.12 ^a	14.7 \pm 0.14 ^b	11.47 \pm 0.20 ^c	14.22 \pm 2.55	142,100	13.5 \pm 0.18 ^a	12 \pm 0.16 ^b	9.58 \pm 0.16 ^c	11.69 \pm 1.98	116,800	15.9 \pm 0.13 ^a	13.6 \pm 0.36 ^b	13.1 \pm 0.17 ^c	14.33 \pm 1.46	143,200
Cd	<0.1	2.4 \pm 0.19 ^a	2.01 \pm 0.14 ^a	1.31 \pm 0.08 ^b	1.92 \pm 0.57	1820	1.14 \pm 0.08 ^a	0.88 \pm 0.06 ^b	0.56 \pm 0.03 ^c	0.86 \pm 0.29	760	0.64 \pm 0.02 ^a	0.47 \pm 0.02 ^b	0.40 \pm 0.01 ^c	0.50 \pm 0.12	400
As	<1.0	29.5 \pm 0.25 ^a	21.4 \pm 0.22 ^b	17.1 \pm 0.18 ^c	22.66 \pm 6.27	2166	18.6 \pm 0.27 ^a	17.2 \pm 0.24 ^b	15.2 \pm 0.26 ^c	17.00 \pm 1.66	1600	19.4 \pm 0.16 ^a	18.7 \pm 0.13 ^b	16.5 \pm 0.11 ^c	18.20 \pm 1.53	1720
Pb	<0.5	15.9 \pm 0.22 ^a	10.7 \pm 0.12 ^b	10.12 \pm 0.18 ^c	12.24 \pm 3.18	2348	1.68 \pm 0.16 ^a	1.39 \pm 0.18 ^b	1.04 \pm 0.09 ^c	1.37 \pm 0.32	174	0.87 \pm 0.03 ^a	0.79 \pm 0.02 ^b	0.73 \pm 0.03 ^c	0.80 \pm 0.07	60
Cu	<1.0	3.9 \pm 0.13 ^a	2.9 \pm 0.10 ^b	1.84 \pm 0.05 ^c	2.89 \pm 1.04	189	1.7 \pm 0.13 ^a	1.03 \pm 0.06 ^b	0.77 \pm 0.03 ^c	1.17 \pm 0.49	17	1.53 \pm 0.1 ^a	1.11 \pm 0.12 ^b	0.93 \pm 0.03 ^c	1.19 \pm 0.31	19
Cr	<1.0	49.3 \pm 0.37 ^a	43.6 \pm 0.32 ^b	41.9 \pm 0.20 ^c	44.91 \pm 3.87	4391	4.28 \pm 0.08 ^a	3.71 \pm 0.15 ^b	1.33 \pm 0.09 ^c	3.11 \pm 1.56	211	1.38 \pm 0.12 ^a	0.99 \pm 0.07 ^b	0.84 \pm 0.03 ^c	1.07 \pm 0.28	7
Zn	<5.0	4.7 \pm 0.17 ^a	3.61 \pm 0.09 ^b	3.00 \pm 0.11 ^c	3.77 \pm 0.89	-25	1.33 \pm 0.1 ^a	1.26 \pm 0.13 ^b	0.78 \pm 0.03 ^c	1.12 \pm 0.30	-78	0.86 \pm 0.02 ^a	0.71 \pm 0.02 ^b	0.55 \pm 0.02 ^c	0.71 \pm 0.16	-86
Fe	<8.0	49.2 \pm 0.24 ^a	45.6 \pm 0.34 ^b	40.97 \pm 0.11 ^c	45.27 \pm 4.15	466	0.97 \pm 0.06 ^a	0.84 \pm 0.04 ^b	0.51 \pm 0.02 ^c	0.77 \pm 0.24	-90	1.41 \pm 0.14 ^a	1.16 \pm 0.14 ^b	1.01 \pm 0.05 ^c	1.19 \pm 0.20	-85
Al	<0.5*	20.3 \pm 0.35 ^a	17.4 \pm 0.27 ^b	16.7 \pm 0.10 ^c	18.14 \pm 1.92	3528	12.7 \pm 0.14 ^a	12.2 \pm 0.24 ^b	10.6 \pm 0.22 ^b	11.84 \pm 1.12	2268	10.0 \pm 0.12 ^a	6.63 \pm 0.14 ^b	4.24 \pm 0.16 ^c	6.97 \pm 2.90	1294
Se	<0.5	0.086 \pm 0.005 ^a	0.068 \pm 0.008 ^b	0.068 \pm 0.0ab08 ^b	0.074 \pm 0.01	-85	0.028 \pm 0.007 ^a	0.023 \pm 0.005 ^a	0.014 \pm 0.005 ^b	0.02 \pm 0.01	-96	0.08 \pm 0.005 ^a	0.07 \pm 0.008 ^a	0.04 \pm 0.008 ^b	0.06 \pm 0.02	-88
Σ	192	162	144	166	56	51	40	49	49	52	45	38	45	38	45	

Table 1. Concentration (mg·L⁻¹; Mean \pm SD) of heavy metals (HM) in water and values of National Environmental Quality Standards (NEQS) in water samples collected from three sites (Indus Delta, Sandpit and, Miani Hor) in three different seasons (monsoon, post-monsoon and pre-monsoon). * taken from ASQG, 2010, not available in NEQS, 1997. ^a p <0.001, ^b p <0.01, ^c p <0.05.

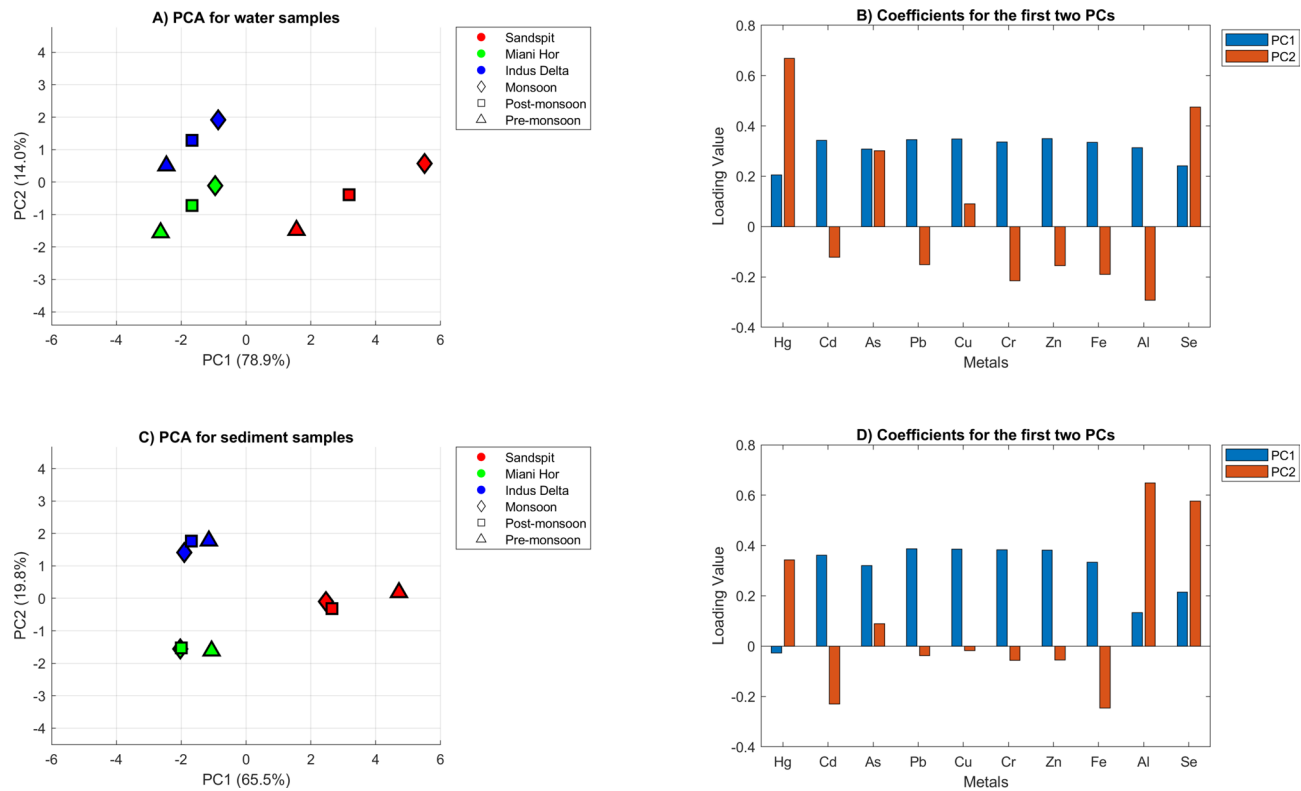


Fig. 2. Principal component analysis of z-scores of elements from Table 1 for elemental water analysis and Table 2 for elemental analysis of sediments at the three mangrove stands.

Hg in total suspended solids (TSS) or total particulate matter (TPM) have shown values as high as $150 \text{ mg}\cdot\text{kg}^{-1}$ in locations with direct anthropogenic interference, especially from industrial activities near coasts, similar to the situation in Karachi^{35–37}. However, little information is available on Hg concentration (in TPM) from the Indian Ocean³⁸, while no work has been reported from the Pakistan coast. In a previous study the TSS levels from Sandspit, Miani Hor, and Indus Delta was observed as 1210–1324, 234–253, and 115–143 $\text{mg}\cdot\text{kg}^{-1}$, respectively (unpublished data).

The Hg pollution index (HPI)'s critical threshold is 100³⁹. Values higher than this threshold indicate inferior water quality. Higher HPI values were observed at Sandspit during the monsoon (138,738), post-monsoon (123,521), and pre-monsoon (96,382) (Supplementary File, Table S2). Miani Hor and Indus Delta also showed a similar seasonal trend but with slightly lower values. At Sandspit, Hg's concentration factor (C_f) was 1147 during pre-monsoon, lower than the Indus Delta (1310) during the same season. The C_f values were corroborated by the water Hg content, which was higher at the Indus Delta ($13.1 \text{ mg}\cdot\text{L}^{-1}$) than at Sandspit ($11.47 \text{ mg}\cdot\text{L}^{-1}$).

Cd, Cu, and Al analysis

The results of MANOVA indicated significant effects of sample types, sites, seasons and their interactions on accumulation of Cd, Cu, and Al (Supplementary File, Table S1). In contrast to Hg, the Cd, Cu, and Al had higher content in all sediment samples (Table 2) compared to water samples (Table 1). The pattern of their contents was also similar across the studied sites. In water, the highest levels of Cd, Cu, and Al were observed during the monsoon and the lowest during the pre-monsoon. However, a reverse pattern was observed in sediment samples. The increased levels of Cd, Cu, and Al in water during subtropical monsoon rains and peak agricultural activities are likely due to farming and industrial run-off. These dissolved metals later accumulate in the sediment during downwelling or winter⁴⁰. In the pre-monsoon, after downwelling (Dec-Feb), the reduced input of fresh water and relatively calm seawater conditions facilitate the chemisorption of Cd, Cu, and Al onto the sediments. However, during upwelling (Jun-Sep), there is desorption of these metals, as reflected in various analyses^{41–43}. The $\% \Delta$ for Cd and Cu was notably higher in Sandspit water (1820 and 189, respectively). Comparatively, Sandspit water was three times more polluted than the other two sites. However, all study sites were found to be slightly above the pollution limits (Supplementary File, Table S3).

The Al concentration in Sandspit water was significantly higher ($\% \Delta$, 3528) than the waters of the other two sites. This difference may be attributed to comparatively low pH (7.25) at Sandspit (unpublished data), which is likely a result of increased anthropogenic activities, leading to the release and increased solubility of Al in the water of Sandspit compared to the other two sites^{7,44}. The Al concentrations of Sandspit water were found to be 14 to 36 times exceeding the NEQS limits²⁷. All the sediment samples collected in the current study appeared to be physically closer to clay, but the content of Al was very low^{18,20,45–48}. Furthermore, the sediment at the Indus Delta showed a high K_d value of 4.69, indicating a rich building capacity for Al at this site.

HM	AVCSR, 2010	Sandspit			Miani Hor			Indus Delta			Average	%Δ [#]	%Δ [#]
		Monsoon	Post-monsoon	Pre-monsoon	Monsoon	Post-monsoon	Pre-monsoon	Monsoon	Post-monsoon	Pre-monsoon			
Hg	0.4	12.8±0.18 ^a	10.8±0.09 ^b	10.1±0.19 ^{bc}	11.24±1.40	2710	11.1±0.19 ^a	10.8±0.09 ^b	8.4±0.11 ^c	10.1±1.46	2425	13.1±0.14 ^a	10.8±0.09 ^c
Cd	0.42	2.8±0.08 ^c	2.9±0.12 ^b	4.2±0.08 ^a	3.31±0.76	688	1.50±0.17 ^c	1.77±0.14 ^b	2.2±0.17 ^a	1.82±0.35	333	0.75±0.01 ^c	0.92±0.03 ^b
As	13	20.5±0.27 ^b	16.8±0.13 ^c	21.8±0.11 ^a	19.70±2.62	51	14.4±0.36 ^b	13.6±0.28 ^c	18.4±0.24 ^a	15.48±2.60	19	16.1±0.12 ^b	15.3±0.12 ^c
Pb	80	21.4±0.30 ^c	25.6±0.24 ^b	31.7±0.22 ^a	26.23±5.20	-67	1.73±0.12 ^c	2.1±0.14 ^b	2.53±0.13 ^a	2.12±0.40	-97.3	1.03±0.06 ^c	1.48±0.11 ^b
Cu	250	4.8±0.08 ^c	5.6±0.12 ^b	6.1±0.16 ^a	5.50±0.65	-97.8	1.82±0.1 ^c	2.02±0.08 ^b	2.23±0.13 ^a	2.02±0.21	-99.2	1.88±0.13 ^b	2.03±0.17 ^b
Cr	90	27.6±0.26 ^c	35.1±0.19 ^b	39.6±0.36 ^a	34.08±6.03	-62	2.59±0.08 ^c	2.86±0.07 ^b	3.21±0.06 ^a	2.89±0.31	-96.8	0.90±0.01 ^c	1.15±0.12 ^b
Zn	165	4.9±0.15 ^c	5.7±0.14 ^b	9.1±0.22 ^a	6.57±2.22	-96.0	1.78±0.13 ^a	1.71±0.11 ^a	1.8±0.1 ^a	1.76±0.05	-98.9	1.08±0.05 ^b	1.11±0.07 ^a
Fe	65,900	2001±11.05 ^a	1822±8.60 ^b	1865±120.5	1772±12.42 ^c	-97.1	1356±11.37 ^a	1292±12.41 ^b	1278±3.79 ^c	1309±41.67	-97.9	1114±11.6 ^a	1045±8.06 ^b
Al	84,900	24.2±0.22 ^c	25.6±0.32 ^b	33.5±0.35 ^a	27.74±5.00	-99.9	13.1±0.21 ^{bc}	13.8±0.16 ^b	17.7±0.17 ^a	14.88±2.47	-99.9	29.1±0.12 ^c	33.2±0.14 ^b
Se	0.17	0.063±0.005 ^b	0.074±0.005 ^b	0.085±0.005 ^a	0.074±0.01	-56	0.022±0.008 ^b	0.026±0.005 ^{a,b}	0.032±0.008 ^a	0.03±0.01	-82	0.06±0.008 ^b	0.08±0.005 ^a
Σ	2120	1950	1928	1999	1404	1341	1335	1360	1178	1112	1082	1124	

Table 2. Concentration (mg·L⁻¹; Mean±SD) of heavy metals (HM) in sediments and Average Values of Clay from Sedimentary Rocks (AVCSR) values in sediment samples collected from three sites (Indus Delta, Sandspit and, Miani Hor) in three different seasons (monsoon, post-monsoon and pre-monsoon). [#]%Δ is calculated by comparing average observed values with the limits described in AVCSR, 2010. ^a $p < 0.001$, ^b $p < 0.01$, ^c $p < 0.05$.

Compared to the other two sites, Cu concentration in Sandspit sediment was higher but still well below the limits defined in Average Values of Clay from Sedimentary Rocks (AVCSR) (Table 2). The higher percentage of Cu in the sediment can be attributed to its easy chemisorption on clay minerals in association with Fe-Mn oxides and hydroxides, which were reportedly present in notable quantities in the studied sediments. The sediments analyzed in this study were rich in Fe (vide infra). The K_d values of Cd (Table 3) at Miani Hor and Indus Delta were comparable (2.12 and 2.00, respectively). In contrast, the K_d value at Sandspit was relatively low (1.72), indicating that Sandspit water is more contaminated due to the influx of anthropogenic Cd²⁵. Cd exhibits similar biogeochemical behavior, whether it accumulates in soil, sediment, organisms, and the aquatic food web^{49,50}. Almost every marine organisms live in or around sediments for most of their life cycle⁵¹. Consequently, most Cd discharged into water bodies either becomes fixed onto sediments or undergo bioaccumulation and biomagnification processes. The K_d value of Cu also indicates that, like Cd, Cu could bind with the sediment, as shown in Table 3³⁰.

Pb and Zn analysis

Lead (Pb) is among the most toxic elements to humans. It gradually accumulates in bones, kidneys, liver, and spleen with age⁵². The results of MANOVA showed significant effects of sample types, sites, seasons and their interactions on concentration of Pb and Zn (Supplementary File, Table S1). Pb also showed the same trend as that of Cd, Cu, and Al, except the values observed in three seasons in the Indus Delta water were very close, i.e., 0.87, 0.79, and 0.73 mg·L⁻¹. Sandspit is highly polluted with Pb as compared to Miani Hor and Indus Delta (Tables 1, 2). The %Δ (2348) in water showed Pb is 25 times higher at Sandspit than other two sites. The K_d for Pb in the pre-monsoon season at Sandspit, Miani Hor, and Indus Delta was higher with respective values of 3.13, 2.43, and 2.38 than the annual average values of K_d in these seasons, 2.14, 1.55, and 1.78, respectively, showing more Pb binding with the sediments. The possible primary Pb sources are agricultural waste running off in the basin⁵³ and auto exhaust emission entering the water basin through atmosphere⁵⁴. Sandspit Beach is thus highly contaminated with Pb, which probably originates from the leaded gasoline, used for decades before getting ban. Up to 10% of Pb in gasoline was released from auto exhausts⁵⁵. In Pakistan, the total number of registered vehicles exceeded 7 million in the year 2022 alone⁵⁶. Thus, Pb found its way into the food web. The higher concentration of Pb at Miani Hor compared to the Indus Delta might be due to barite excavation in the vicinity²². Similarly, Zn also shows the same trend as Cd, Cu, and Al. However, a considerable and interpretable difference was not observed in the three seasons among the concentration in sediments at Miani Hor (1.78, 1.71, and 1.80) and Indus delta (1.08, 1.11, and 1.74) (Table 2). The study correlates strongly with the recommendation of Pulford et al.⁴⁵, Hooda⁴⁹, and Ramos et al.⁵⁷.

Zn showed similar biogeochemical behavior in sediments like Pb and Cd. High Fe content (vide infra), which may also occlude Zn in the lattice structures, could be a possible reason for the high retention of Zn in sediments. Various phosphate fertilizers contain Zn and Cd and other elements as micronutrients. Such fertilizers increase the P, Cd, and Zn concentrations in the fertilized land and marine sediments via run-off⁵⁸. The K_d for Zn is also > 1 (Table 3) and is related to the clay and CaCO_3 content. Thus, a higher concentration of Pb and Zn is associated mainly with oxides of Fe-Mn, as these are capable of forming stable complexes^{30,45,46}.

Se and Cr analysis

Selenium—a micronutrient for various organisms, is one of the elements with the narrowest gap between deficiency and toxicity. Se can accumulate in the body of marine fish and animals. HM toxicity adversely affects marine biota⁵⁹. In this study, MANOVA showed only site specific and type x season—specific effects on Se concentration (Supplementary File, Table S1). The concentration of Se was found to be low (ranging from 0.01 to 0.08 mg·L⁻¹) irrespective of season and sites (Tables 1, 2). Overall, the trend of Se was similar to Cd, Cu, and Al. All values of Se were found to be less than NEQS²² and AVCSR limits⁶⁰.

MANOVA indicated significant effects of sample types, sites, seasons and their interactions on accumulation of Cr (Supplementary File, Table S1). The seasonal concentration trend for Cr was similar to Cd, Cu, Al, Pb, and Zn. Its concentration was higher in water than in sediments, irrespective of sites and seasons, except for the Cr concentration, which was slightly higher at Indus delta, in post- and pre-monsoon and at Miani Hor in Pre-monsoon. Samples of water and sediment from Sandspit contained manifold higher concentrations of Cr as compared to the Miani Hor and Indus Delta (Tables 1, 2). Sandspit received more Cr from Lyari River and Korangi Creek, which are receiving industrial waste from dozens of tanneries. The %Δ with NEQS²⁷ was 4391 in water at Sandspit, roughly 45 times higher than Miani Hor and Indus delta. Cr at the Indus Delta was 3 times more than the NEQS limits²².

Cr (VI) compounds are usually more easily soluble, mobile, and bioavailable, which maximizes their toxic effect and more availability in water. Similarly more oxidized form of Chromium (Cr IV) is also very soluble and is not adsorbed strongly to suspended particles, and hence sediments in natural waters⁶¹. Most physicochemical behavior discussed for Cu (vide supra) also stands true for Co, including binding to clay⁶¹.

As and Fe analysis

Arsenic (As) is a carcinogen and one of the hazardous elements for almost all biotas⁵². Excessive iron (Fe) has severe effects on the gastrointestinal tract and biological fluids⁶². MANOVA analysis demonstrated that sample type, site, season, and their interactions significantly influenced As and Fe accumulation (Supplementary File, Table S1). Like Hg and Cr, the overall concentration of As was higher in water than in sediment (%Δ being 2166, 1720, and 1600 in water at Sandspit, Indus Delta, and Miani Hor, respectively). The trends of concentrations of As were similar to Hg, Cd, Cu, Al, Pb, Zn, Cr, and Se in water (Table 1). In the case of sediments, the highest As was observed in pre-monsoon, which gradually decreased to a minimum in post-monsoon (Table 2). Concentrations of inorganic As in some estuaries and coastal waters facing anthropogenic interference have been reported to

HM	Sandspit					Miani Hor					Indus Delta				
	C _f	Er ⁱ	EF	I _{geo}	K _d	C _f	Er ⁱ	EF	I _{geo}	K _d	C _f	Er ⁱ	EF	I _{geo}	K _d
Monsoon															
Al	-	-	0.012489	-12.11	1.19	-	-	0.005764	-13.606	1.03	-	-	0.020214	-12.08	2.91
As	1.367	13.667	57.84424	0.072	0.69	0.907	9.067	50.14749	-0.52	0.77	1.073	10.733	72.26212	-0.276	0.83
Cd	2.800	84.000	244.5448	2.152	1.17	1.500	45.000	171.1968	1.252	1.32	0.750	22.500	104.1934	0.252	1.17
Cr	0.307	0.613	11.24906	-2.29	0.56	0.029	0.058	1.379466	-5.704	0.61	0.010	0.020	0.570517	-7.261	0.64
Cu	0.112	0.560	0.82167	-6.065	1.23	0.036	0.182	0.348968	-7.687	1.07	0.038	0.188	0.438779	-7.64	1.23
Fe	-	-	1	-5.782	40.67	-	-	1	-6.168	1397.94	-	-	1	-6.452	790.07
Hg	51.200	2048.000	1173.815	4.415	0.78	44.400	1776.000	1330.199	4.209	0.82	52.400	2096.000	1910.907	4.448	0.82
Pb	0.306	1.529	9.812359	-2.487	1.35	0.025	0.124	1.036597	-6.12	1.03	0.015	0.074	0.751234	-6.864	1.18
Se	-	-	13.59381	-2.017	0.73	-	-	6.203366	-3.535	0.79	-	-	20.59352	-2.087	0.75
Zn	0.029	0.029	1.111567	-5.629	1.04	0.008	0.008	0.386386	-7.54	1.34	0.006	0.006	0.381916	-7.84	1.26
RI		2148					1830					2129			
Post-monsoon															
Al	-	-	0.010872	-12.266	1.47	-	-	0.008265	-13.15	1.13	-	-	0.024584	-11.89	5.01
As	1.120	11.200	46.10318	-0.215	0.79	0.960	9.600	55.72755	-0.437	0.79	1.020	10.200	73.20574	-0.35	0.82
Cd	3.000	90.000	254.822	2.252	1.44	1.770	53.100	212.019	1.49	2.01	0.920	27.600	136.2497	0.546	1.96
Cr	0.390	0.780	13.91328	-1.943	0.81	0.032	0.064	1.598727	-5.561	0.77	0.013	0.026	0.79479	-6.875	1.16
Cu	0.096	0.480	0.684962	-6.288	1.93	0.040	0.202	0.406502	-7.536	1.96	0.041	0.203	0.505072	-7.529	1.83
Fe	-	-	1	-5.742	39.96	-	-	1	-6.238	1538.10	-	-	1	-6.544	900.86
Hg	43.200	1728.000	963.2272	4.16	0.73	43.200	1728.000	1358.359	4.17	0.90	46.000	1840.000	1788.278	4.261	0.83
Pb	0.366	1.829	11.41603	-2.229	2.39	0.030	0.150	1.320627	-5.837	1.51	0.021	0.106	1.150718	-6.341	1.87
Se			14.27003	-1.907	1.09	-	-	7.694409	-3.294	1.13	-	-	29.27104	-1.672	1.14
Zn	0.033	0.033	1.232412	-5.44	1.58	0.010	0.010	0.52139	-7.177	1.36	0.010	0.010	0.655937	-7.152	1.56
RI		1832					1791					1878			
Pre-monsoon															
Al	-	-	0.012955	-11.876	2.01	-	-	0.010717	-12.802	1.67	-	-	0.027351	-11.787	8.42
As	1.453	14.533	54.47276	0.161	1.27	1.227	12.267	71.98748	-0.084	1.21	1.153	11.533	85.64356	-0.173	1.05
Cd	4.200	126.000	324.8376	2.737	3.21	2.200	66.000	266.4133	1.804	3.93	1.330	39.900	203.7954	1.078	3.33
Cr	0.440	0.880	14.29285	-1.769	0.95	0.036	0.071	1.814032	-5.394	2.41	0.017	0.034	1.079758	-6.482	1.80
Cu	0.122	0.610	0.792604	-5.942	3.32	0.045	0.223	0.453678	-7.394	2.90	0.045	0.224	0.576634	-7.387	2.41
Fe	-	-	1	-5.607	43.25	-	-	1	-6.253	2505.88	-	-	1	-6.593	1000.00
Hg	61.200	2448.000	1242.504	4.672	0.88	33.720	1348.800	1071.89	3.812	0.88	43.200	1728.000	1737.624	4.17	0.82
Pb	0.453	2.264	12.87169	-1.92	3.13	0.036	0.181	1.60847	-5.568	2.43	0.025	0.124	1.399752	-6.108	2.38
Se	-	-	16.24188	-1.585	1.25	-	-	9.573783	-2.994	2.29	-	-	30.28538	-1.672	2.00
Zn	0.052	0.052	1.791528	-4.765	3.03	0.010	0.010	0.554844	-7.103	2.31	0.006	0.006	0.429043	-7.814	3.16
RI		2592					1427					1779			
Average of three seasons at three sites															
Al	-	-	0.01	-12.08	1.53	-	10.31	0.01	-13.19	1.26	-	-	0.02	-11.92	4.69
As	1.31	13.13	52.81	0.01	0.87	1.03	54.70	59.29	-0.35	0.91	1.08	10.82	77.04	-0.27	0.89
Cd	3.33	100.00	274.73	2.38	1.72	1.82	0.06	216.54	1.52	2.12	1.00	30.00	148.08	0.63	2.00
Cr	0.38	0.76	13.15	-2.00	0.76	0.03	0.20	1.60	-5.55	0.93	0.01	0.03	0.82	-6.87	1.10
Cu	0.11	0.55	0.77	-6.10	1.90	0.04	-	0.40	-7.54	1.74	0.04	0.21	0.51	-7.52	1.72
Fe	-	-	1.00	-5.71	41.20	-	1617.60	1.00	-6.22	1700.00	-	-	1.00	-6.53	887.39
Hg	51.87	2074.67	1126.52	4.42	0.79	40.44	0.15	1253.48	4.06	0.86	47.20	1888.00	1812.27	4.29	0.82
Pb	0.38	1.87	11.37	-2.21	2.14	0.03	-	1.32	-5.84	1.55	0.02	0.10	1.10	-6.44	1.78
Se	-	-	14.70	-1.84	1.00	-	0.01	7.82	-3.27	1.50	-	-	26.72	-1.81	1.17
Zn	0.04	0.04	1.38	-5.28	1.75	0.01	0.008	0.49	-7.27	1.57	0.01	0.01	0.49	-7.60	1.85
RI		2191					1683					1929			

Table 3. Contamination Factor (C_f), Potential Ecological Risk Indices (Erⁱ), Enrichment Factors (EF), Geo-accumulation Factor (I_{geo}), and the partition coefficient (K_d) of heavy metals (HM) in sediment samples collected from three sites (Indus Delta, Sandspit and, Miani Hor) in three different seasons (monsoon, post-monsoon and pre-monsoon).

be higher than those in the open ocean, primarily due to progressive mixing of As-poor fresh water with As-rich seawater^{29,63}. Indus alluvial plains are naturally eroded by rains, groundwater suction, drilling, mining, irrigation networks, etc. As a result, the water and sediment of the Indus River became rich through the process of mineralization. Ultimately, the rivers lead these minerals to marine sink^{41,47}.

Moreover, calcite depositions and mineralized carbonates in the sediment and sampling sites and adjoining areas are potential arsenic sinks⁶⁴. An average K_d (0.87 to 0.91) also supports more As in the water than in sediments. However, the pre-monsoon season reflected the K_d ranging from 1.05 to 1.27, justifiable by the low tides and downwelling. Fe was remarkably high in sediments of Pakistan's coasts compared to water. The concentration patterns were similar in water and sediment, irrespective of seasons and sites. In water, it followed the trend of Cd, Cu, Al, Pb, Zn, and Se; in sediment, its trend was individual to sampling sites and seasons (Tables 1, 2). The analyzed HM concentration of Fe was exceptionally high, with an average of 1865 (%Δ 466), 1309, and 1056 mg·kg⁻¹ in sediment at Sandspit, Miani Hor, and Indus Delta, respectively.

Fe is the most common lithogenic element⁶⁵ and is present in considerably lower amounts in water bodies. Therefore, it accumulates in the sediment through terrestrial run-off. The oxides and oxy-hydroxides of Fe are reported to chemisorb considerable quantities of Zn, Cd, and Pb in its lattice^{45,57}. These Fe compounds also influence sediments' physico-chemical properties, e.g., aggregate stabilization, cementing effect, phosphorus, etc., by buffering the soil systems⁶⁶. Barite contains Fe_2O_3 as the main impurity, which is ultimately dumped into the sea⁶⁷. Compared to the surrounding marine bodies, the relatively higher content of Fe in Sandspit water may be attributed to large steel mills, mines, and ship-breaking industries in the adjoining areas. The suspended load of Fe-oxide dust in seawater have been reported between 250 and 300 mg·L⁻¹⁶⁸. The Fe content at Miani Hor and Indus Delta was ~ 6 times higher than the NEQS limits²⁷ in water while at Sandspit it is exceeding 10 ~ 11 times (Table 1).

Interestingly, the Fe content is still low, confirming that the sediment at Sandspit is neither pure clay nor sand. This needs a separate comprehensive study to assess risk elements, organic matter, clay content, concentration of Fe- and/or Mn-oxides, etc.^{45,46,69}. Pakistan is rich in minerals, including barite. Its production has recently been increased to 75,000 metric tons per year, ranking Pakistan at 8th position globally²². Barite is rich with Pb (galena), Hg (cinnabar), As (orpiment, realgar, niccolite), etc., and also contains < 10% impurities, including alumina (Al_2O_3)⁶⁷. These HM are contributed through natural erosion as well as by anthropogenic activity.

Spatio-Temporal Trends

Spatial variations

The MANOVA results demonstrated the significant effects of sample site along with its interactions with sample type and season on HM concentrations across Sandspit, Miani Hor, and the Indus Delta (Supplementary File, Table S1). These effects indicating that pollution levels were not uniform in studied sites, instead varied due to differences in natural geochemical properties, hydrodynamic conditions, and anthropogenic influences. Sandspit exhibited the highest levels of Hg, Pb, Cd, and As (Tables 1, 2), reflecting industrial discharge, domestic wastewater influx, and mining activities. These findings confirm our hypothesis that Sandspit would be the most polluted site. In contrast, Miani Hor, with its alluvial and clay-rich sediment, showed moderate HM retention, influenced by agricultural runoff and mining residues. The Indus Delta displayed relatively lesser HM concentration, with increased levels of Hg, Cr, and As during the monsoon due to riverine input and tidal mixing.

Different indices from Table 3 and Supplementary Table S1 and S2 consistently identify Sandspit as the most polluted site. In water samples, C_f was highest for Hg, Cd, and Cr, while PLI and HPI for Hg and Cd confirmed extreme contamination. Higher values of C_d and mC_d further emphasized its pollution severity. In sediments, C_f peaked for Cd, Hg, and As, with higher E_{ri} for Hg highlighting environmental threats. The EF value was exceptionally high for Cd and Hg, while I_{geo} for Cd confirmed substantial pollution. Additionally, K_d suggest high Hg mobility and stronger Al retention at Sandspit.

Temporal variations

The MANOVA reveals that HM accumulation is significantly influenced by season with strong interaction effects among other factors (Supplementary File, Table S1). The cumulative HM content in the water and sediment during the three seasons was highest during the monsoon season (Tables 1, 2), and it was found to decrease gradually from post-monsoon to pre-monsoon season. These findings rejects the first hypothesis that HM concentrations would be highest during the pre-monsoon season, as it is the driest season. Instead, the elevated levels observed during the monsoon season were likely influenced by strong tides, wave action, and terrestrial and river runoff. The highest average of HM content was observed in water samples of Sandspit (166 mg·L⁻¹), as expected from water bodies around megacities. It was 50 and 44 mg·L⁻¹ at Miani Hor and Indus Delta, respectively. Except for a few HM (Tables 1, 2), HM content in sediment was highest in pre-monsoon. The type of sediment and composition plays an important role in HM retention. In general, coarse-grained soils exhibit a lower tendency for HM adsorption than fine-grained soils, owing to larger surface areas. Clay minerals, Fe-Mn oxides and oxyhydroxides, humic acids, and other organic coatings (bearing cation exchange capacity) display enhanced adsorption properties⁷⁰⁻⁷². Mangrove stands at Sandspit are also rich in litter. Except for Fe and Zn, all HM followed the similar trends in sediments as that of adjoining water. Fe and Hg in the sediment of Miani Hor showed concentration order as monsoon > post-monsoon > pre-monsoon. In contrast, other HM showed a general order of concentration as monsoon < post-monsoon < pre-monsoon. Like Miani Hor, Fe, and Hg in the sediment of Indus Delta showed similar order from monsoon > post-monsoon > pre-monsoon while all the other HM showed mixed trends.

The HPI (Supplementary File, Table S2) and C_f were calculated separately for each metal. Total Heavy Metal Pollution Indices (Σ HPI), Pollution Load Indices (PLI), Contamination Degrees (Cd), and of Modified

Contamination Degrees (mCd) provide a collective measure of HM pollution in the study area (Supplementary File, Table S2). These parameters indicate that water quality at these sites, particularly at Sandspit, is severely affected by HM pollution. Among the analyzed HM, As, Cd, and Hg exhibited notably high EF values, while the I_{geo} values also reflected higher contamination levels (Table 3). These elevated values suggest that these HM are primarily introduced into the natural environment through anthropogenic activities, such as industrial discharge, terrestrial run-off and other human-induced sources.

Conclusions

This study highlights significant HM contamination in water and sediments at Sandspit, Miani Hor, and the Indus Delta, with Sandspit showing the highest pollution levels due to industrial discharge and waste influx. Seasonal variations, especially during the monsoon, intensified HM mobilization, further deteriorating water quality. Statistical analyses confirmed site-specific and seasonal influences on HM distribution, emphasizing the need for regular monitoring and remediation. The excessive Hg levels surpass national and international safety limits, posing ecological and public health risks. The long-term retention of Cd, Cu, and Al in sediments suggests persistent contamination affecting mangrove vegetation and associated marine biodiversity. High HM concentrations adversely affect mangrove ecosystems, exerting stress on *A. marina*, the only species managing to survive in heavily polluted areas. In addition, these ecological disruptions threaten coastal resilience, fisheries, and the overall health of marine habitats. Immediate action is needed to regulate industrial waste, improve pollution control, and develop sustainable remediation strategies to safeguard coastal ecosystems of Pakistan.

Data availability

All data generated or analysed during this study are included in this published article (and its Supplementary Information files).

Received: 24 June 2024; Accepted: 6 May 2025

Published online: 23 August 2025

References

1. Rahman, S. U. et al. Adaptation and remediation strategies of mangroves against heavy metal contamination in global coastal ecosystems: A review. *J. Clean. Prod.* **441**, 140868. <https://doi.org/10.1016/j.jclepro.2024.140868> (2024).
2. Faizan, M. et al. Phytochelatins: Key regulator against heavy metal toxicity in plants. *Plant Stress* **11**, 100355. <https://doi.org/10.1016/j.stress.2024.100355> (2024).
3. Lohano, H. D. & Maqbool, M. B. Ocean governance and integrated ocean management. In *The Blue Economy* (eds Hazra, S. & Bhukta, A.) 309–319 (Springer, 2022). https://doi.org/10.1007/978-3-030-96519-8_17.
4. Siddiqui, P. J. A., Farooq, S., Shafique, S. & Farooqui, Z. Conservation and management of biodiversity in Pakistan through the establishment of marine protected areas. *Ocean Coast. Manag.* **51**(5), 377–382. <https://doi.org/10.1016/j.ocecoaman.2008.01.006> (2008).
5. Haider, S. W., Kazmi, S. J. H., Arsalan, M., Naseem, S. & Kanwal, H. Spatial evaluation of precipitation patterns in the catchment area of Malir River during monsoon spells of 2019 through geospatial techniques. *Arab. J. Geosci.* **15**, 1435. <https://doi.org/10.1007/s12517-022-10574-9> (2022).
6. Farooqui, Z. et al. Assessment of litter production in semi-arid mangroves forests near active Indus river mouth (Hajambro Creek) and Karachi backwaters. *Pak. J. Bot.* **44**(5), 1763–1768 (2012).
7. Rizvi, S.N. Status of marine pollution in the context of coastal zone management in Pakistan. In *Coastal zone management imperative for maritime developing nations* (ed. Haq, B.U., Haq, S.M., Kullenberg, G., Stel, J.H.). Coastal Zone Management Imperative for Maritime Developing Nations. Coastal Systems and Continental Margins, vol 3. 347–370 (Springer Dordrecht, 1997). https://doi.org/10.1007/978-94-017-1066-4_19.
8. Azizullah, A., Khattak, M. N. K., Richter, P. & Häder, D. P. Water pollution in Pakistan and its impact on public health—A review. *Environ. Int.* **37**(2), 479–497. <https://doi.org/10.1016/j.envint.2010.10.007> (2011).
9. Saifullah, S. M. & Rasool, F. Mangroves of miani hor lagoon on the north Arabian Sea coast of Pakistan. *Pak. J. Bot.* **34**(3), 303–310 (2002).
10. Qureshi, M. T. Rehabilitation and management of mangrove forests of Pakistan. In *Towards the rational use of high salinity tolerant plants* (eds Liebth, H. & Al Masoom, A. A.) 89–95 (Springer, 1993). https://doi.org/10.1007/978-94-011-1858-3_8.
11. Jayakumar, M., Surendran, U., Raja, P., Kumar, A. & Senapathi, V. A review of heavy metals accumulation pathways, sources and management in soils. *Arab. J. Geosci.* **14**(20), 2156. <https://doi.org/10.1007/s12517-021-08543-9> (2021).
12. Yin, H., Gao, Y. & Fan, C. Distribution, sources and ecological risk assessment of heavy metals in surface sediments from Lake Taihu. *China. Environ. Res. Lett.* **6**(4), 044012. <https://doi.org/10.1088/1748-9326/6/4/044012> (2011).
13. Karbasdehi, V. N. et al. Data on metal contents (As, Ag, Sr, Sn, Sb, and Mo) in sediments and shells of *Trachycardium lacunosum* in the northern part of the Persian Gulf. *Data Brief* **8**, 966–971. <https://doi.org/10.1016/j.dib.2016.06.065> (2016).
14. Marchand, C., Fernandez, J. M. & Moreton, B. Trace metal geochemistry in mangrove sediments and their transfer to mangrove plants (New Caledonia). *Sci. Total Environ.* **562**, 216–227. <https://doi.org/10.1016/j.scitotenv.2016.03.206> (2016).
15. Cheng, H. et al. Metal (Pb, Zn and Cu) uptake and tolerance by mangroves in relation to root anatomy and lignification/suberization. *Tree Physiol.* **34**(6), 646–656. <https://doi.org/10.1093/treephys/tpu042> (2014).
16. Chan, M. W. H., Hasan, K. A., Balthazar-Silva, D., Mirani, Z. A. & Asghar, M. Evaluation of heavy metal pollutants in salt and seawater under the influence of the Lyari River and potential health risk assessment. *Mar. Pollut. Bull.* **166**, 112215. <https://doi.org/10.1016/j.marpolbul.2021.112215> (2021).
17. USEPA, 3051A; Element, C.A.S., Method 3051A microwave-assisted acid digestion of sediments, sludges, soils, and oils. *Z. Für Anal. Chem.* **111**, 362–366 (2007). http://www.wipp.energy.gov/library/Information_Repository_A/Supplemental_Information/EPA%20Method%203051.pdf.
18. Syed, N. A., Siddiqua, T. & Sohoo, N. Evaluation of morphodynamics of Miani Hor Coastal Lagoon of Lasbela, Baluchistan, Pakistan. *Oceanol* **225**, 1–11 (2019).
19. Petrovský, E., Kapička, A., Jordanova, N. & Borůvka, L. Magnetic properties of alluvial soils contaminated with lead, zinc and cadmium. *J. Appl. Geophys.* **48**(2), 127–136. [https://doi.org/10.1016/S0926-9851\(01\)00085-4](https://doi.org/10.1016/S0926-9851(01)00085-4) (2001).
20. Holmes, D. A. & Western, S. Soil texture patterns in the alluvium of the lower Indus plains. *J. Soil Sci.* **20**(1), 23–37. <https://doi.org/10.1111/j.1365-2389.1969.tb01551.x> (1969).
21. Liao, R. et al. Three-dimensional assessment of heavy metal contamination in soil affected by urbanization at the urban-rural interface of Chengdu. *Emerg. Contam.* **11**, 100482. <https://doi.org/10.1016/j.emcon.2025.100482> (2025).

22. Shahab, B., Bashir, E., Kaleem, M., Naseem, S. & Rafique, T. Assessment of barite of Lasbela, Balochistan, Pakistan, as drilling mud and environmental impact of associated Pb, As, Hg. *Cd and Sr. Environ. Earth. Sci.* **75**(14), 1115. <https://doi.org/10.1007/s12665-016-5916-7> (2016).
23. Iqbal, A. R. Environmental issues of Indus River Basin: An analysis. *ISSRA Papers J. Govern. Public Policy* **5**(1), 91–112 (2013).
24. Naidoo, G., Hiralal, T. & Naidoo, Y. Ecophysiological responses of the mangrove *Avicennia marina* to trace metal contamination. *Flora* **209**, 63–72. <https://doi.org/10.1016/j.flora.2013.10.003> (2014).
25. Sofawi, A. B., Nazri, M. N. & Rozainah, M. Z. Nutrient variability in mangrove soil: Anthropogenic, seasonal and depth variation factors. *Appl. Ecol. Environ. Res.* **15**, 1983–1998. https://doi.org/10.15666/aeer/1504_19831998 (2017).
26. Bat, L., & Özkan, E. Y. Heavy metal levels in sediment of the turkish black sea coast. In *Oceanography and coastal informatics: Breakthroughs in research and practice* (ed. Information Resources Management Association) 86–107 (IGI Global, 2019). <https://doi.org/10.4018/978-1-5225-7308-1.ch004>.
27. NEQS, (National Environmental and Quality Standards) Pakistan Environmental Legislation and the National Environmental Quality Standards, Government of Pakistan.
28. Gworek, B., Bemowska-Kalabun, O., Kijeńska, M. & Wrzosek-Jakubowska, J. Mercury in marine and oceanic waters—A review. *Water Air Soil Pollut.* **227**(10), 371. <https://doi.org/10.1007/s11270-016-3060-3> (2016).
29. Byrd, J. T. Comparative geochemistries of arsenic and antimony in rivers and estuaries. *Sci. Total Environ.* **97**, 301–314. [https://doi.org/10.1016/0048-9697\(90\)90247-R](https://doi.org/10.1016/0048-9697(90)90247-R) (1990).
30. Merrikhpour, H. & Jalali, M. Geostatistical assessment of solid-liquid distribution coefficients (Kd) for Cd, Cu, Pb, and Zn in surface soils of Hamedan, Iran. *Model. Earth Syst. Environ.* **1**(4), 1–9. <https://doi.org/10.1007/s40808-015-0048-8> (2015).
31. Hamza, S. et al. Factorial analysis of trace elements of *Tamarindus indica* with reference to Bela ophiolite. *Intl. J. Basic Appl. Sci.* **3**(3), 166–171. <https://doi.org/10.14419/ijbas.v3i3.2580> (2014).
32. Hasan, A. B. et al. Trace metals pollution in seawater and groundwater in the ship breaking area of Sitakund Upazilla, Chittagong, Bangladesh. *Mar. Pollut. Bull.* **71**(1–2), 317–324. <https://doi.org/10.1016/j.marpolbul.2013.01.028> (2013).
33. Kumar, S. C., Jaikumar, M., Robin, R. S., Karthikeyan, C. & Kumar, S. Heavy metal concentration of seawater and marine organisms in Ennore Creek, southeast coast of India. *J. Toxicol. Health.* **103**, 192–201 (2013).
34. Mohiuddin, S. & Naqvi, I. I. Marine sediment's profile for mercury as pollution indicator at Karachi coast. *Int. J. Econ. Environ. Geol.* **5**, 15–24 (2014).
35. Hosek, M. et al. Persistent mercury hot spot in Central Europe and Skalka Dam reservoir as a long-term mercury trap. *Environ. Geochem. Health* **42**, 1273–1290. <https://doi.org/10.1007/s10653-019-00408-1> (2019).
36. Wilken, R. & Hintelmann, H. Mercury and methylmercury in sediments and suspended particles from the river Elbe, North Germany. *Water, Air, Soil, Pollut.* **56**, 427–437. <https://doi.org/10.1007/BF00342289> (1991).
37. Cranston, R. E. & Buckley, D. E. Mercury pathways in a river and estuary. *Environ. Sci. Technol.* **6**(3), 274–278. <https://doi.org/10.1021/es60062a007> (1972).
38. Chakraborty, P. et al. Seawater intrusion and resuspension of surface sediment control mercury (Hg) distribution and its bioavailability in water column of a monsoonal estuarine system. *Sci. Total Environ.* **660**, 1441–1448. <https://doi.org/10.1016/j.scitotenv.2018.12.477> (2019).
39. Prasad, B. & Bose, J. Evaluation of the heavy metal pollution index for surface and spring water near a limestone mining area of the lower Himalayas. *Environ. Geol.* **41**, 183–188. <https://doi.org/10.1007/s002540100380> (2001).
40. Thilagavathi, B. et al. Heavy metal distribution in sediments of Muthupettai mangroves, southeast coast of India. *J. Ocean. Uni. China* **10**(4), 385–390. <https://doi.org/10.1007/s11802-011-1807-4> (2011).
41. Cao, Y. Z., Wang, S., Zhang, G., Luo, J. & Lu, S. Chemical characteristics of wet precipitation at an urban site of Guangzhou. *South China. Atmos. Res.* **94**(3), 462–469. <https://doi.org/10.1016/j.atmosres.2009.07.004> (2009).
42. Ding, C. et al. Competitive sorption of Pb (II), Cu (II) and Ni (II) on carbonaceous nanofibers: a spectroscopic and modeling approach. *J. Hazard. Mater.* **313**, 253–261. <https://doi.org/10.1016/j.jhazmat.2016.04.002> (2016).
43. Zang, F. et al. Immobilization of Cu, Zn, Cd and Pb in mine drainage stream sediment using Chinese loess. *Chemosphere* **181**, 83–91. <https://doi.org/10.1016/j.chemosphere.2017.04.070> (2017).
44. Angel, B. M. et al. Metal concentrations in the waters and sediments of Port Curtis, Queensland. CSIRO Wealth from Oceans Flagship Technical Report. 1–75 (2012). <https://www.dceew.gov.au/sites/default/files/env/pages/884f8778-caa4-4bd9-b370-318518827db6/files/09gcc-important2.pdf>.
45. Pulford, I. D. & Bakhsh, A. Uptake of zinc by soil: adsorption or precipitation. In *Proceedings of the international conference on heavy metals in the environment* (Vol. 2, pp. 193–196) (1989).
46. Turekian, K. K. & Wedepohl, K. H. Distribution of the elements in some major units of the earth's crust. *Geol. Soc. Am. Bull.* **72**(2), 175–192. [https://doi.org/10.1130/0016-7606\(1961\)72\[175:DOTEIS\]2.0.CO;2](https://doi.org/10.1130/0016-7606(1961)72[175:DOTEIS]2.0.CO;2) (1961).
47. Giosan, L. et al. On the control of climate-and human-modulated fluvial sediment delivery on river Delta development: The Indus. In AGU Fall Meeting Abstracts (2006, December).
48. Ahmed, Y.Z. Microbial Community and its role in ecosystem (Doctoral Dissertation, University of Karachi), pp. 1–257 (2016).
49. Hooda, P.S. Trace elements in soils. Chester UK. 596 (John Wiley & Sons Ltd; West Sussex, UK, 2010). <https://eprints.kingston.ac.uk/id/eprint/23918>.
50. Wesner, J. S. et al. Metamorphosis affects metal concentrations and isotopic signatures in a mayfly (*Baetis tricaudatus*): Implications for the aquatic-terrestrial transfer of metals. *Environ. Sci. Tech.* **51**(4), 2438–2446. <https://doi.org/10.1021/acs.est.6b05471> (2017).
51. Fletcher, D. E., Lindell, A. H., Stillings, G. K., Blas, S. A. & McArthur, J. V. Trace element accumulation in lotic dragonfly nymphs: Genus matters. *PLoS ONE* **12**(2), 1–27. <https://doi.org/10.1371/journal.pone.0172016> (2017).
52. Jomova, K., Alomar, S. Y., Nepovimova, E., Kuca, K. & Valko, M. Heavy metals: toxicity and human health effects. *Arch. Toxicol.* **99**, 153–209. <https://doi.org/10.1007/s00204-024-03903-2> (2024).
53. Monbet, P. Mass balance of lead through a small macrotidal estuary: The Morlaix River estuary (Brittany, France). *Mar. Chem.* **98**, 59–80. <https://doi.org/10.1016/j.marchem.2005.08.003> (2006).
54. Chen, H., Yan, Y., Hu, D., Peng, L. & Wang, C. High contribution of vehicular exhaust and coal combustion to PM2.5-bound Pb pollution in an industrial city in North China: An insight from isotope. *Atmos. Environ.* **294**, 119503. <https://doi.org/10.1016/j.atmosenv.2022.119503> (2023).
55. USEPA. Integrated science assessment for lead (final report). EPA/600/R-10/075F. Washington, DC (2013). <https://cfpub.epa.gov/ncea/isa/recordisplay.cfm?deid=255721>.
56. CEIC Data. Number of registered vehicles in Pakistan. CEIC <https://www.ceicdata.com/en/indicator/pakistan/number-of-registered-vehicles> (Accessed 24 Feb 2025).
57. Ramos, L., Hernandez, L. M. & Gonzalez, M. J. Sequential fractionation of copper, lead, cadmium and zinc in soils from or near Donana National Park. *J. Environ. Qual.* **23**(1), 50–57. <https://doi.org/10.2134/jeq1994.00472425002300010009x> (1994).
58. Lambert, R., Grant, C. & Sauvé, S. Cadmium and zinc in soil solution extracts following the application of phosphate fertilizers. *Sci. Tot. Environ.* **378**(3), 293–305. <https://doi.org/10.1016/j.scitotenv.2007.02.008> (2007).
59. Karthikeyan, P., Marigoudar, S. R., Nagarjuna, A. & Sharma, K. V. Toxicity assessment of cobalt and selenium on marine diatoms and copepods. *Environ. Chem. Ecotoxicol.* **1**, 36–42. <https://doi.org/10.1016/j.enceco.2019.06.001> (2019).
60. Wang, N. et al. Supplementation of micronutrient selenium in metabolic diseases: its role as an antioxidant. *Oxid. Med. Cell Longev.* 1–13 (2017). <https://doi.org/10.1155/2017/7478523>.

61. Jabłońska-Czapla, M. Arsenic, antimony, chromium, and thallium speciation in water and sediment samples with the LC-ICP-MS technique. *Int. J. Anal. Chem.* 1–13 (2015). <https://doi.org/10.1155/2015/171478>.
62. Guzman, F. T., Gonzalez, F. J. A. & Martinez, R. R. Implementing Lecane quadridentata acute toxicity tests to assess the toxic effects of selected metals (Al, Fe, and Zn). *Ecotoxicol. Environ. Safety* 73(3), 287–295. <https://doi.org/10.1016/j.ecoenv.2009.10.006> (2010).
63. Ho, H. H., Swennen, R., Cappuyns, V., Vassilieva, E. & Van Tran, T. Necessity of normalization to aluminum to assess the contamination by heavy metals and arsenic in sediments near Haiphong Harbor. *Vietnam. J. Asian Earth Sci.* 56, 229–239. <https://doi.org/10.1016/j.jseas.2012.05.015> (2012).
64. Edmunds, W. M., Ahmed, K. M. & Whitehead, P. G. A review of arsenic and its impacts in groundwater of the Ganges–Brahmaputra–Meghna Delta, Bangladesh. *Environ. Sci. Proc. Imp.* 17(6), 1032–1046. <https://doi.org/10.1039/x0xx00000x> (2015).
65. Korte, L. F. et al. Downward particle fluxes of biogenic matter and Saharan dust across the equatorial North Atlantic. *Atmos. Chem. Phys.* 17(9), 6023–6040. <https://doi.org/10.5194/acp-17-6023-2017> (2017).
66. Monterroso, C., Macías, F., Alvarez, E. & Fernández-Marcos, M. L. Geochemistry of aluminium and iron in mine soils from As Pontes, Galicia (NW Spain). *Water Air Soil Pollut.* 110(1–2), 81–102. <https://doi.org/10.1023/A:1005055704392> (1999).
67. Ozmar, K. E. & Hicyilmaz, C. Concentration of barite and fluorite minerals Eskisehir–Beylikahir District. *Fizykochem Probl Mineralurgii (Physicochem. Probl. Miner. Process)* 28, 65–74 (1994).
68. Saifullah, S. M., Ismail, S., Khan, S. H. & Saleem, M. Land use—Iron pollution in mangrove habitat of Karachi, Indus Delta. *Earth Interact.* 8(17), 1–9 (2004).
69. Naidoo, G. & Raiman, F. Some physical and chemical properties of mangrove soils at Sipingo and Mgeni. *Natal. S. Afr. J. Bot.* 1(4), 85–90. [https://doi.org/10.1016/S0022-4618\(16\)30155-3](https://doi.org/10.1016/S0022-4618(16)30155-3) (1982).
70. Elliott, H. A., Liberati, M. R. & Huang, C. P. Competitive adsorption of heavy metals by soils. *J. Environ. Qual.* 15(3), 214–219. <https://doi.org/10.2134/jeq1986.00472425001500030002x> (1986).
71. Crawford, R. J., Harding, I. H. & Mainwaring, D. E. Adsorption and coprecipitation of single heavy metal ions onto the hydrated oxides of iron and chromium. *Langmuir* 9(11), 3050–3056. <https://doi.org/10.1021/la00035a051> (1993).
72. Kalbitz, K. & Wennrich, R. Mobilization of heavy metals and arsenic in polluted wetland soils and its dependence on dissolved organic matter. *Sci. Total Environ.* 209(1), 27–39. [https://doi.org/10.1016/S0048-9697\(97\)00302-1](https://doi.org/10.1016/S0048-9697(97)00302-1) (1998).

Acknowledgements

The authors sincerely thank the Ongoing Research Funding program, (ORF-2025-194), King Saud University, Riyadh, Saudi Arabia.

Author contributions

MWHC: Methodology, Formal analysis, Investigation, Writing—Original Draft, MI: Methodology, Formal analysis, Writing—Original Draft, MQ: Conceptualization, Validation, Visualization, Writing—Review & Editing, MHS: Funding acquisition, Writing—Review & Editing, SA: Funding acquisition, Writing—Review & Editing, PJAS: Resources, Funding acquisition, SG: Visualization, Writing—Review & Editing, MA: Visualization, Writing—Review & Editing, TTH: Visualization, Writing—Review & Editing, MFW: Visualization, Writing—Review & Editing, ATA: Funding acquisition, MR: Conceptualization, Resources, Supervision, Project administration, Validation, Writing—Review & Editing.

Declarations

Competing interest

The author(s) declare no competing interests.

Additional information

Supplementary Information The online version contains supplementary material available at <https://doi.org/10.1038/s41598-025-01712-w>.

Correspondence and requests for materials should be addressed to M.R.

Reprints and permissions information is available at www.nature.com/reprints.

Publisher's note Springer Nature remains neutral with regard to jurisdictional claims in published maps and institutional affiliations.

Open Access This article is licensed under a Creative Commons Attribution-NonCommercial-NoDerivatives 4.0 International License, which permits any non-commercial use, sharing, distribution and reproduction in any medium or format, as long as you give appropriate credit to the original author(s) and the source, provide a link to the Creative Commons licence, and indicate if you modified the licensed material. You do not have permission under this licence to share adapted material derived from this article or parts of it. The images or other third party material in this article are included in the article's Creative Commons licence, unless indicated otherwise in a credit line to the material. If material is not included in the article's Creative Commons licence and your intended use is not permitted by statutory regulation or exceeds the permitted use, you will need to obtain permission directly from the copyright holder. To view a copy of this licence, visit <http://creativecommons.org/licenses/by-nc-nd/4.0/>.

© The Author(s) 2025